University of
Reading

Effects of coastal managed retreat on mercury biogeochemistry

Article

Accepted Version

It is advisable to refer to the publisher's version if you intend to cite from the work.

www.reading.ac.uk/centaur

CentAUR

Central Archive at the University of Reading

1   <u>Effects of coastal managed retreat on mercury biogeochemistry</u>

2

3   Tom Sizmur[a*], Adam Godfrey[a] and Nelson J. O'Driscoll[a]

4

5   [a]Department of Earth & Environmental Science, K.C. Irving Environmental Science Center,

6   Acadia University, Wolfville, NS, B4P 2R6, Canada.

7

8   *Corresponding author

9   Present address: Soil Research Centre, Department of Geography and Environmental Science,

10   Russell Building, University of Reading, Reading, RG6 6DW, UK

11   E-mail: t.sizmur@reading.ac.uk

12   Phone: +44(0)118 3788913

13

14   **Abstract**

15   We investigated the impact of managed retreat on mercury (Hg) biogeochemistry at a site subject

16   to diffuse contamination with Hg. We collected sediment cores from an area of land behind a

17   dyke one year before and one year after it was intentionally breached. These sediments were

18   compared to those of an adjacent mudflat and a salt marsh. The concentration of total mercury

19   (THg) in the sediment doubled after the dyke was breached due to the deposition of fresh

20   sediment that had a smaller particle size, and higher pH. The concentration of methylmercury

21   (MeHg) was 27% lower in the sediments after the dyke was breached. We conclude that coastal

22   flooding during managed retreat of coastal flood defences at this site has not increased the risk of

23   Hg methylation or bioavailability during the first year. As the sediment becomes vegetated,

24   increased activity of Hg-methylating bacteria may accelerate Hg-methylation rate.

25   **Keywords:** Mercury, Methylmercury, Biogeochemistry, Sediment deposition, Coastal

26   **Capsule:** Mercury concentration doubled in sediments after coastal flooding but methylmercury
27   concentration deceased

Introduction

Coastal wetlands have been subject to dramatic global declines in the past due to dyking and draining for agriculture. However, this practice is now being reversed in many countries because salt marshes are valued as habitats for wildlife and as natural defence against rising sea-levels (Singh et al., 2007). Managed retreat of coastal defences has led to an increase in the number of sites where dykes are breached, agricultural fields are inundated with seawater, sediment is deposited over soils, and new salt marshes are created. Inundation of previously dyked farmland leads to considerable biogeochemical changes, characterised by increased salinity, lower redox potential (Portnoy and Giblin, 1997) and a decaying mat of buried vegetation (Emmerson et al., 2000). There is concern that biogeochemical changes during managed retreat may alter the fate of redox-sensitive contaminants such as mercury (Hg) (Morris et al., 2014).

The Bay of Fundy in Southeastern Canada is renowned for having the largest tidal amplitude in the world, which gives rise to expansive intertidal mudflats and vast areas of salt marsh (Crowell et al., 2011; Desplanque and Mossman, 2004). For centuries the Bay's coastline has been extensively dyked to use the land for agriculture (Wynn, 1979). The land surrounding the Bay of Fundy is designated a 'biological mercury hotspot' due to elevated concentrations of Hg in biota (Evers et al., 2007). The Bay of Fundy itself has been identified as an area of special concern for Hg contamination because the Bay's ecosystem may be critical to concentrations of Hg found in fish, birds and wildlife (Hung and Chmura, 2006).

49   Mercury enters the Bay of Fundy through seawater inflow and atmospheric deposition

50   (Sunderland et al., 2012). The Hg present in sediments of the Bay of Fundy is strongly

51   associated with organic matter and fine textured sediments (O'Driscoll et al., 2011; Sizmur et al.,

52   2013b). Inorganic Hg in sediments can be converted to methylmercury (MeHg) under anoxic

53   conditions by sulphate-reducing bacteria (Compeau and Bartha, 1985). Methylmercury can

54   biomagnify through food webs (Lavoie et al., 2010) and is a potent neurotoxin affecting higher

55   trophic level animals and humans (Rasmussen et al., 2005).

56

57   Increases in MeHg concentrations in sediments and biota have been observed during the decades

58   that follow terrestrial freshwater flooding for dam construction or wetland creation (Kelly et al.,

59   1997; Sinclair et al., 2012). However, little research has been done to assess changes in Hg

60   biogeochemistry after coastal wetland flooding. Terrestrial flooding events, like reservoir or

61   wetland creation, entail a permanent change in sediment redox from oxic to anoxic conditions

62   because the sediments are constantly flooded. However, coastal flooding events subject the land

63   to fluctuating oxic/anoxic conditions due to the tidal cycle. These fluctuations generate an oxic-

64   anoxic interface in the sediment. The temporal fluctuations in redox conditions increases the

65   volume of sediment where sulphate reduction and mercury methylation may occur (Heim et al.,

66   2007; Sizmur et al., 2013a). However, there is also frequent tidal flushing of inundated areas

67   which acts as a significant means of removing MeHg from the surface of coastal sediments

68   (Guédron et al., 2012). Therefore, it is not clear if managed retreat will increase or decrease Hg

69   and MeHg concentrations in sediments.

70

71 We investigated the effects of managed retreat on mercury biogeochemistry at Beaubassin

72 Research Station where a dyke has recently been breached, allowing the seawater to inundate

73 land previously drained for agriculture.

74

75 **Materials and Methods**

76 *Site Description*

77 Beaubassin Research Station (Latitude: 45.852195 Longitude: -64.279631) is located on the

78 Chignecto Isthmus between Nova Scotia and New Brunswick, Canada (Figure 1a). It lies along

79 the Cumberland Basin, a branch of Chignecto Bay, in the Bay of Fundy which is sourced from

80 the Gulf of Maine. The average tidal amplitude at Beaubassin is 11 m (Gordon Jr and Baretta,

81 1982). Recently, an eroding 150-year-old dyke was replaced with a new dyke built

82 approximately 90 m back from the pre-existing coastline in order to protect transport

83 infrastructure and the historic site of Fort Beausejour from tidal surges. The 40 ha of low lying

84 land between the old dyke and the new dyke (Latitude: 45.851595 Longitude: -64.294379) was

85 flooded in October 2010. Flooding occurred when the old dyke was deliberately breached so that

86 sediment could accumulate to protect the new dyke before the old dyke completely failed

87 (Ollerhead et al., 2011). Tidal re-entry has resulted in the rapid deposition of fresh sediment over

88 the top of the agricultural soil, burying a mat of terrestrial vegetation. At the time of sampling,

89 new salt marsh vegetation was yet to establish.
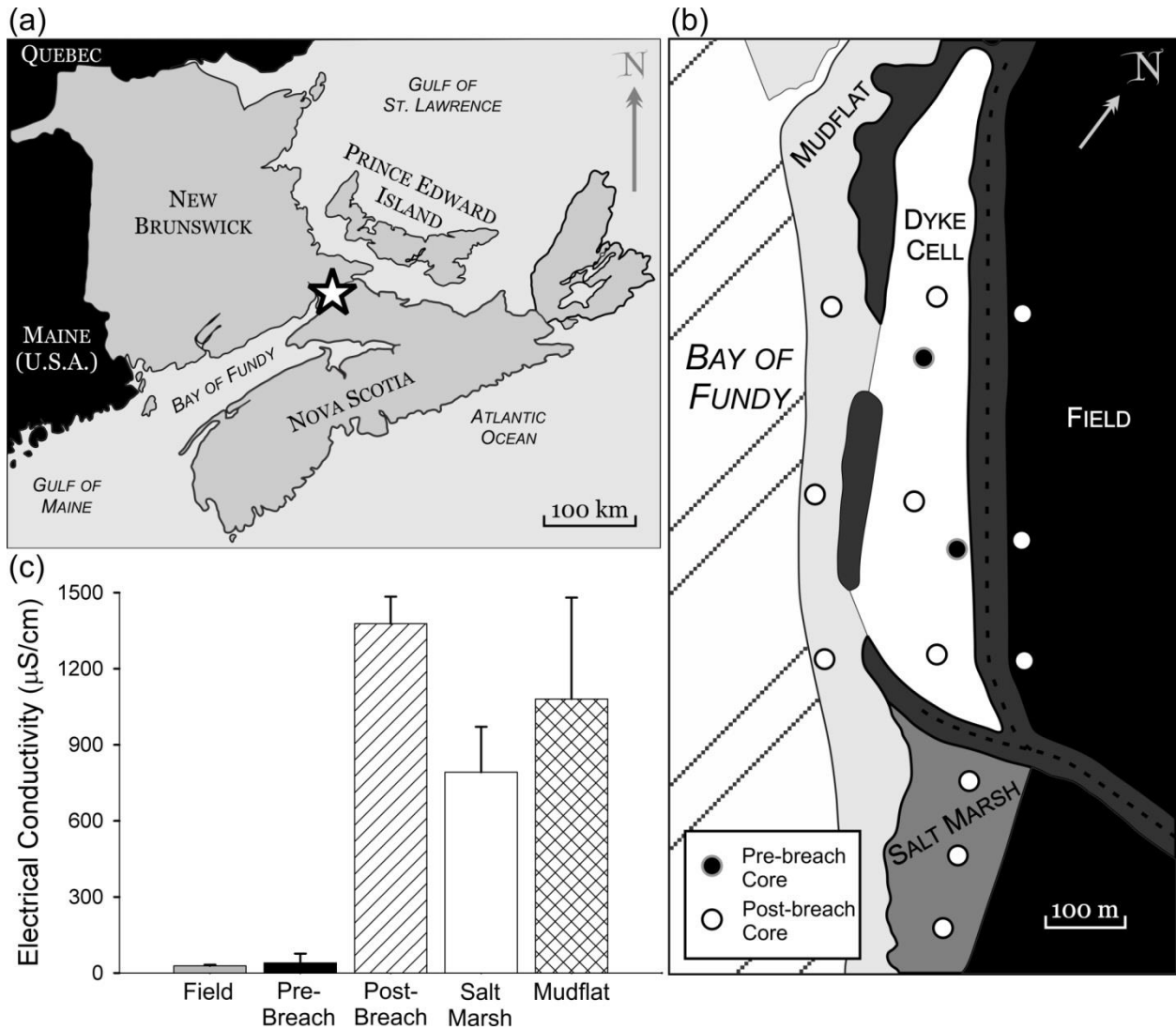
Figure 1. (a) Site location at Beaubassin, New Brunswick, Canada; (b) Location of all cores sampled from the dyke cell (pre-breach and post-breach) along with adjacent sites (mudflat, salt marsh and field). The location of two gaps in the wall of the dyke cell represent where they were deliberately breached in 2010; (c) Electrical conductivity of sediment cores sampled (averaged 0-15 cm) shown here to demonstrate the influence of seawater on the dyke cell pre-breach and post-breach.

Sample Collection and Preparation

99   Two 16 cm deep cores were taken in the dyke cell (Figure 1b) between the new and the old

100 dykes (hereafter referred to as the pre-breach cores) in summer 2009 (before the old dyke was

101 breached in 2010). We returned to the site in summer 2011 to collect cores one year after the old

102 dyke was breached. Three 15 cm deep cores were sampled at four locations: (i) The area

103 previously sampled in the dyke cell between the new and old dykes (hereafter referred to as the

104 post-breach cores), (ii) the mudflat seaward of the dyke cell, (iii) a pre-existing salt marsh

105 adjacent to the dyke cell, and (iv) the field landward of the dyke cell (Figure 1b). All cores were

106 sampled at low tide using polyvinyl chloride (PVC) cores (10 cm internal diameter) that were

107 dug out with a stainless steel spade.

108

109 Pre-breach cores were sliced in 2 cm intervals to a depth of 16 cm, producing a total of eight

110 slices per core. Each of the post-breach, mudflat, salt marsh, and field cores were sliced at 1 cm

111 intervals for the upper 5 cm of sediment and then at 2 cm intervals for the remaining 10 cm,

112 producing a total of 10 core slices per core. Core slices were individually sealed in Ziploc bags at

113 the research station and placed in a dark cooler with ice packs for transport back to the

114 laboratory.

115

116 At the laboratory each sediment slice was thoroughly homogenised by hand in the Ziploc bag

117 and frozen as a wet homogenate at -20 ˚C. Sediment samples were later thawed and a subsample

118 dried at 60 ^{o}C for 24 hours. Dried sediment samples were ground with a pestle and mortar and

119 sieved to < 2 mm. A subsample of wet sediment was analysed for electrical conductivity (EC)

120 using a VWR Symphony SP90M5 meter and Orion electrical conductivity probe. The field was

121 only sampled to demonstrate that the pre-breach sediments had not been inundated by seawater

122 prior to the breach. Since the EC of the pre-breach and field cores (Figure 1c) revealed no

123 significant difference ($p > 0.05$), further analysis of the field cores was deemed unnecessary.

124 Each slice of the remaining cores was analysed for total mercury (THg), MeHg, percentage

125 organic matter (%OM), particle size distribution, water-extractable organic carbon (WEOC) and

126 pH.

127

128 *Analytical Procedures*

129 Total mercury in sediment was determined using thermal degradation – gold amalgamation

130 atomic absorbance spectroscopy as outlined in EPA Method 7473 (1998) using a Nippon MA-

131 2000 non-dispersive double-beam cold-vapor atomic absorption Hg analyzer. Methylmercury

132 was determined in sediments by alkaline digestion, ethylation purge and trap Gas

133 Chromatography - Cold Vapour Atomic Fluorescence Spectrometry (GC-CVAFS) following

134 Sizmur et al (2013b). A 100 mg sample of sediment was digested in 2.5 ml of basic methanol (25

135 % KOH/MeOH) by shaking on a reciprocal shaker for 1 hour and then heating for 1 hour at 90

136 ^{o}C. Within 24 hours of digestion, a 60 µl aliquot was transferred to a glass reaction bubbler,

137 ethylated with $NaB(C_2H_5)_4$, purged with argon, collected on a Tenax trap and analysed for MeHg

138 using GC-AFS (Brooks Rand Model III).

139

140 Organic matter in sediment was determined by loss on ignition at 500 ^{o}C (Byers et al., 1978) and

141 particle size distribution by the micro-pipette method (Miller and Miller, 1987). Sand was

142 calculated as particles 2000-63 μm, silt as 63-2 μm, and clay as < 2 μm in diameter. Water-

143 extractable organic carbon was determined following Sizmur et al (2011) by shaking 1 g of

144 sediment with 40 ml of Milli Q water for 2 hours on a reciprocal shaker at 120 shakes min^{-1},

145 followed by centrifuging at 4000 rpm (2647 G) for 20 min and filtering to < 0.45 μm with

146 polypropylene membrane filters, before TOC/TIC analysis with a Shimadzu TOC-V CPH Total

147 Organic Carbon Analyzer. Sediment pH was analysed in WEOC vials prior to centrifuging.

148

149 *Quality control*

150 Sediments were analysed in triplicate alongside certified reference materials MESS-3 (National

151 Research Council Canada) and SQC-1238 (Sigma Aldrich RTC) for THg and MeHg

152 respectively. Mean recovery of THg from MESS-3 was 102.2 % (SD = 1.4 %). Mean recovery of

153 MeHg from SQC-1238 was 94.4 % (SD = 12.0 %). Detection limits for MeHg and THg were

154 0.65 and 1.21 pmol g^{-1}, respectively. Both samples and reference materials during Hg analysis

155 were corrected for background by subtracting averaged method blanks from the analysed

156 samples.

157 *Statistical Analysis*

158 Statistical analysis was carried out using Genstat version 16. Normality and homoscedasticity

159 was assessed by inspecting residual plots. Two-way analysis of variance was carried out on all

160 data (MeHg, THg, pH, clay, %OM, WEOC and EC) using 'site' and 'depth' as the factors and

161 allowing for interactions. Fisher's least significant difference was used to identify differences

162 between individual treatments. Multiple linear regression was carried out by forward selection;

163 first the variable that resulted in the highest R^2 values was included in the model, then variables

164   that resulted in the greatest increase were added. Data presented in text as average values at each

165   site are calculated from the concentrations in cores averaged across all depths. All the raw data is

166   provided in the supporting information.

167

168   **Results**

169   *Mercury and Methylmercury*

170   The average concentration of THg in the post-breach cores was 85.1 pmol g^{-1} (SD = 15.6) which

171   was approximately double the concentration in the pre-breach cores (41.1 pmol g^{-1}, SD = 9.52).

172   THg decreased significantly ($p < 0.001$) with depth (Table 1) in the post-breach and mudflat

173   cores but this decrease was not observed in the pre-breach or the salt marsh cores (Figure 2). The

174   THg concentration in the salt marsh cores was significantly ($p < 0.05$) greater than the mudflat or

175   the dyke cell pre- or post-breach. The post-breach cores had significantly ($p < 0.05$) greater Hg

176   concentrations than the pre-breach cores.

177   Table 1 Analysis of variance from physiochemical sediment variables; Water Extractable
178   Organic Carbon (WEOC), pH, Electrical Conductivity (EC), Clay content and Organic Matter
179   (OM).

Variable	Site F value	Depth F value	Site-depth interaction F value
THg	62.19***	2.34*	0.41
MeHg	12.83***	2.06*	0.55
% MeHg	31.41***	0.95*	0.62
% OM	15.03***	0.29	0.93
pH	16.87***	0.97*	0.79
% Clay	24.93***	1.74	0.38
WEOC	32.14***	1.68	1.36
EC	69.15***	0.82	1.23

180   * = $p < 0.05$, *** = $p < 0.001$

181
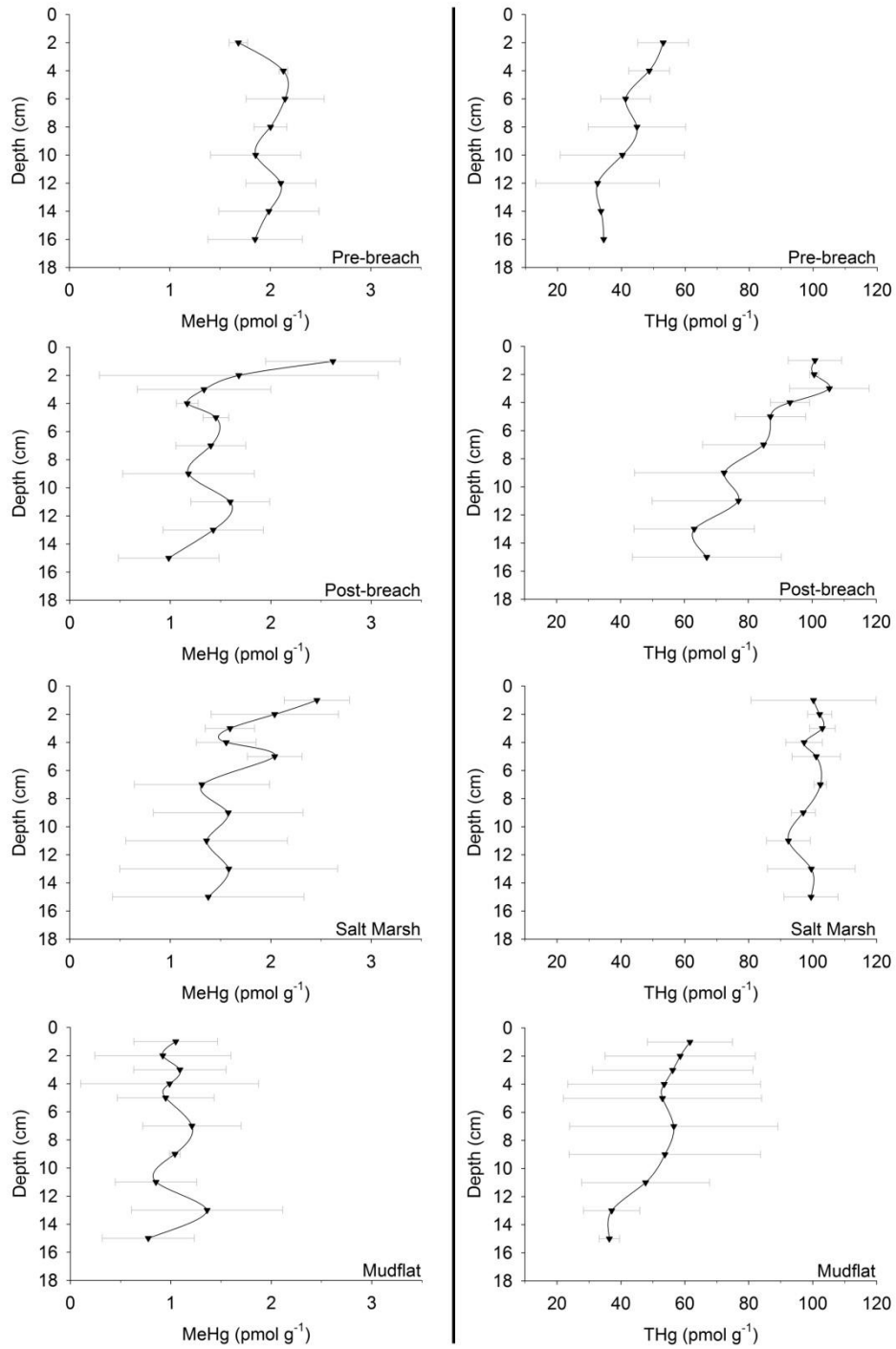
Figure 2. Total mercury (THg) and methylmercury (MeHg) concentrations of sediment slices of cores sampled from the dyke cell (pre-breach and post-breach) along with adjacent sites (mudflat and salt marsh). The error bars represent the standard deviation of three replicate cores (n = 2 for the pre-breach cores).

186   MeHg significantly ($p < 0.05$) decreased with depth (Table 1) in the post-breach and salt marsh

187   cores (Figure 2). Although THg was greater after inundation, MeHg concentration was

188   significantly ($p < 0.05$) lower in post-breach sediments (Figure 2). Methylmercury

189   concentrations were 27% lower in the post-breach cores (1.48 pmol g^{-1}, SD = 0.54) compared to

190   the pre-breach cores (1.97 pmol g^{-1}, SD = 0.31). However, we did measure 36% higher MeHg

191   concentrations in the upper 2 cm of the post-breach sediment than in the top 2 cm of the pre-

192   breach cores (Figure 2). The post-breach MeHg concentration was not significantly ($p > 0.05$)

193   different than that measured in the salt marsh (1.69 pmol g^{-1}, SD = 0.60) but was significantly (p

194   > 0.05) greater than MeHg in the mudflat (1.02 pmol g^{-1}, SD = 0.51). The percentage of MeHg

195   as a proportion of the THg (%MeHg) was significantly ($p < 0.05$) greater in the pre-breach cores

196   (5.97%, SD = 2.99) than the post-breach cores (2.02%, SD = 0.58). %MeHg in the post-breach

197   sediment was not significantly ($p > 0.05$) different from the mudflat (2.34%) or salt marsh

198   (1.84%) sediments.

199

200   *Physiochemical variables*

201   The EC of the pre-breach cores was not significantly different to the samples taken from the field

202   behind the new dyke. EC was significantly increased ($p < 0.05$) by periodic tidal inundation of

203   the dyke cell, increasing over 2000% from pre- to post-breach (Figure 1c). Post-breach sediment

204   EC was also significantly ($p < 0.05$) greater than the salt marsh and mudflat but the magnitude of

205   the difference was much smaller.

206

207   Sediment pH was significantly ($p < 0.001$) greater after inundation of the dyke cell, rising from

208   5. 08 (SD = 1.2) in the pre-breach cores to 7.43 (SD = 0.6) in the post-breach cores (Figure 3).

209   There was no significant ($p > 0.05$) pH difference between the post-breach cores and the salt

210   marsh or mudflat cores.

211

212   The texture of the sediment in the top 15 cm of the dyke cell significantly ($p < 0.001$) changed

213   during salt marsh restoration as fresh sediment with a smaller particle size distribution was

214   deposited over the top of the drained agricultural field (Figure 3). Percentage clay was

215   significantly ($p < 0.05$) greater and sand significantly ($p < 0.05$) lower in the sediment after the

216   inundation. Percentage clay in the post-breach cores (29.8%, SD = 1.52) was nearly double that

217   in the pre-breach cores (16.6%, SD = 13.8). The proportions of sand, silt and clay in the post-

218   breach cores were not significantly ($p > 0.05$) different to the sediments sampled from the

219   mudflat (Figure 3) but clay content was significantly ($p < 0.05$) greater than sediments sampled

220   from the salt marsh.

221

222   The post-breach sediments had significantly ($p < 0.05$) higher organic matter (%OM) and WEOC

223   than the pre-breach cores (Table 1 and Figure 3). There was no significant ($p > 0.05$) difference

224   between the post-breach cores and the salt marsh and mudflat cores, for either %OM or WEOC.

225   The concentration of both WEOC (44.9 mmol kg^{-1}, SD = 4.64) and %OM (6.3%, SD = 0.8) in

226   the post-breach cores was greater than the mudflat cores (32.1 mmol kg^{-1}, SD = 8.87 and 5.8%,

227   SD = 1.2) but lower than the salt marsh cores (47.9mmol kg^{-1}, SD = 7.17 and 6.7%, SD = 0.7).

228
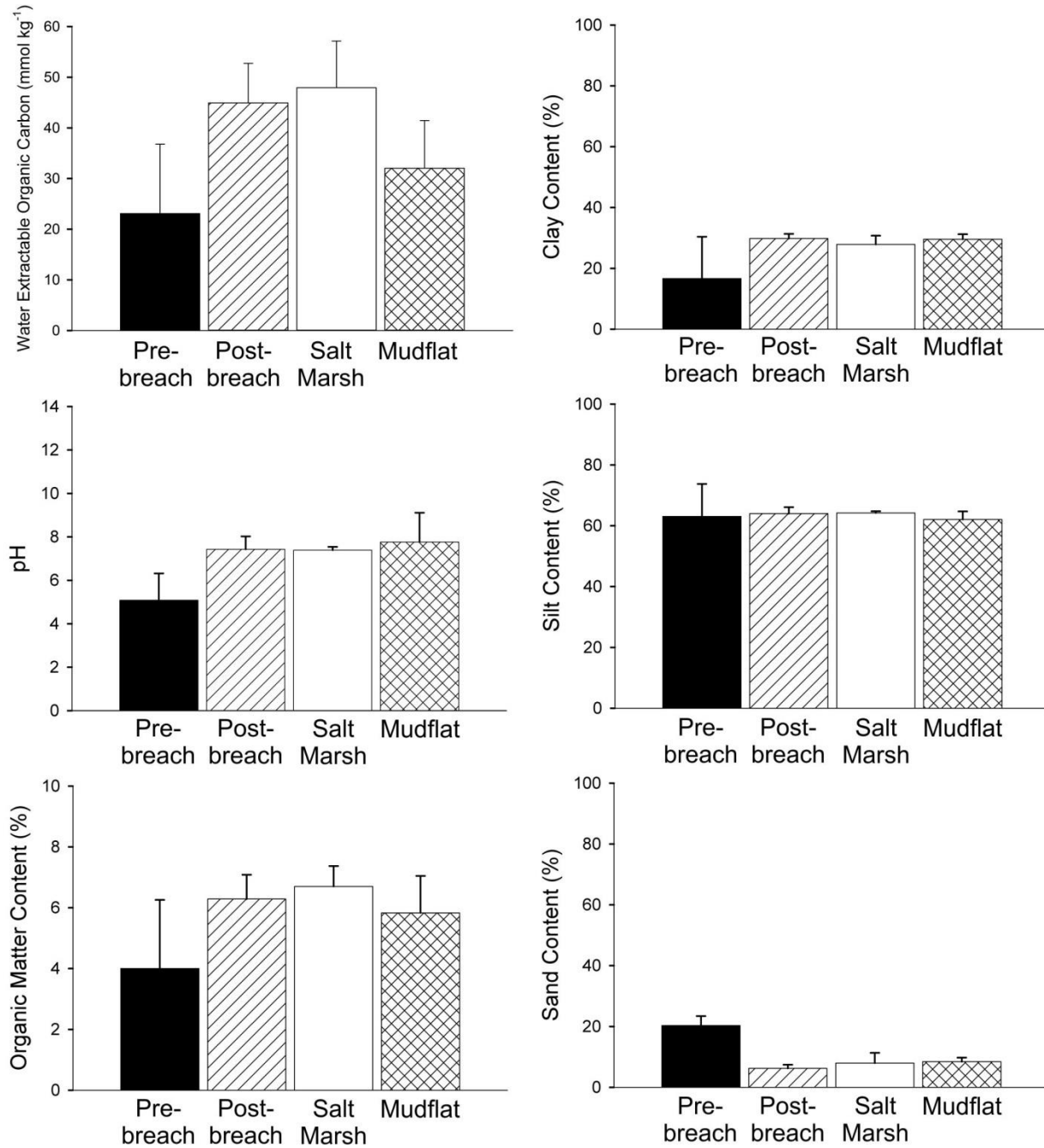
Figure 3. Physiochemical variables measured in cores (averaged 0-15 cm) sampled
from the dyke cell (pre-breach and post-breach) along with adjacent sites (mudflat and
salt marsh). The error bars represent standard deviation of three replicate cores (n = 2
for the pre-breach cores).

233

234 *Multiple linear regressions*

235 The correlation between the best multiple linear regression model and the THg concentrations

236 measured in the sediments (Figure 4) yielded an R^2 value of 0.524 and a p value < 0.001 (Table

237 2). The explanatory variables in order of decreasing importance were WEOC, pH, EC and

238 %Clay. Adding the next most important variable (%OM) decreased the R^2 value to 0.519.

239 WEOC alone explained 36.7% of the variation in the observed data.

240 Table 2 Significance and correlation results of forward multiple linear regression models for the
241 prediction of THg and MeHg from physiochemical sediment variables; Water Extractable
242 Organic Carbon (WEOC), pH, Electrical Conductivity (EC), Clay content and Organic Matter
243 (OM).

Response variable	Fitted terms	F value	R^2
THg	WEOC	61.8***	0.367
	WEOC+pH	48.6***	0.476
	WEOC+pH+EC	35.5***	0.496
	WEOC+pH+EC+Clay	29.9***	0.524
MeHg	EC	7.02**	0.54
	EC+THg	8.36***	0.123
	EC+THg+pH	7.07***	0.148
	EC+THg+pH+Clay	6.05***	0.161
	EC+THg+pH+Clay+WEOC	5.50***	0.176
	EC+THg+pH+Clay+WEOC+OM	6.56***	0.241

244 ** = p < 0.01, *** = p < 0.001

245 The variability in MeHg concentrations was more difficult to explain than the THg

246 concentrations using the physiochemical variables measured. The multiple linear regression

247 model for MeHg (Figure 4) had a lower R^2 value than the model for THg. The fit which included

248 EC, THg, pH, %Clay, WEOC and %OM (in order of decreasing importance) had an R^2 value of

249 0.241 and a p value of < 0.001. Although EC accounted for the greatest extent of the variability

250 in the MeHg dataset, when considered on its own EC accounted for only 5.4% of the variation.

251 This indicates that variables that we measured could not adequately explain the concentration of

252 MeHg in the sediments.
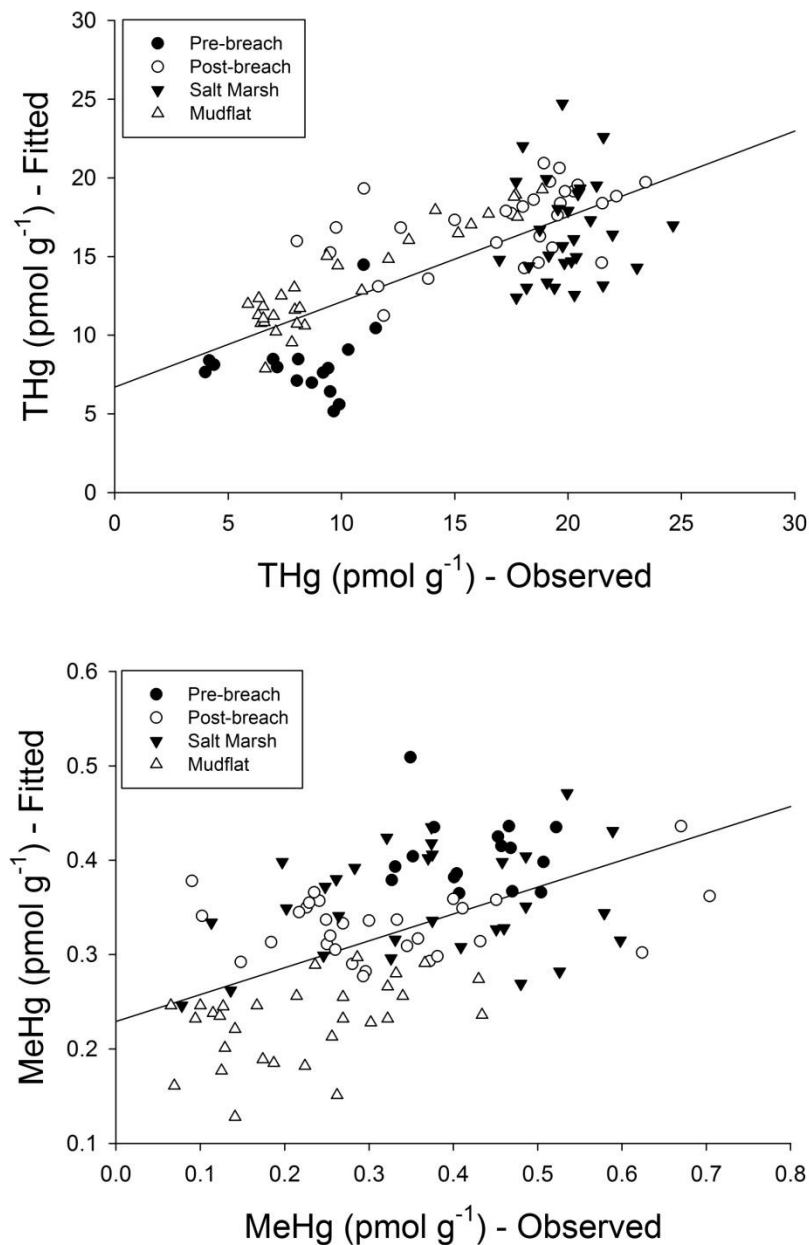
Figure 4. Total mercury (THg) and methylmercury (MeHg) concentrations observed in
cores sampled from the dyke cell (pre-breach and post-breach) along with adjacent
sites (mudflat and salt marsh) plotted against fitted THg and MeHg concentrations that
were predicted using multiple linear regression models (Table 2) created with the same
data. The THg model included WEOC, pH, EC, and %Clay as explanatory variables,
explaining 51.9% of the variability. The MeHg model included EC, THg, pH, %Clay,
WEOC and %OM as explanatory variables, explaining 24.1% of the variability.

Discussion

Post-breach sediments are chemically more similar to the salt marsh and mudflat than pre-breach sediments

The breaching of the dyke and inundation of the dyke cell deposited a large quantity of fresh sediment over the top of the pre-existing soil. This event changed the biogeochemistry of the system by increasing the EC, pH, %OM and WEOC. The impact of this change is best demonstrated by the considerable increase in the EC observed (Figure 1c) as the dyke cell changed from a terrestrial environment to a coastal environment due to inundation with saline water. While the topography of the mudflat and the salt marsh gently slopes down towards the sea, the soil in the dyke cell was relatively flat prior to breaching and inundation. The deposition of fresh sediment in the dyke cell was unevenly distributed leaving puddles of seawater which we observed in depressed areas at low tide. Evaporation of water and precipitation of salts in these depressed areas (Mouneimne and Price, 2007) has resulted in the EC of the post-breach sediments being elevated above levels measured in the mudflat or the salt marsh (Figure 1c).

The objective of the managed retreat is for salt marsh vegetation to colonise the freshly deposited sediment once the depth of the sediment raises the wetland to an elevation high enough for vegetation to survive (Williams and Orr, 2002). During the post-breach sampling in 2011 the dyke cell was still unvegetated and looked more similar to a mudflat than a salt marsh. This observation is supported by the textural analysis of the sediment deposited in the dyke cell (post-breach) which was similar to the sediment sampled from the mudflat (Figure 3). The chemistry of the post-breach sediments (WEOC, pH and %OM) was more similar to the salt marsh and

283   mudflat sediments than the samples collected pre-breach. However, this data must be interpreted

284   with caution since only two cores were collected prior to the dyke being breached.

285

286

287   *Post-breach sediments have greater total Hg but lower MeHg concentrations*

288   The total Hg concentrations in the reclaimed region were similar to those found in other studies

289   of non-vegetated intertidal mudflats (O'Driscoll et al., 2011; Sizmur et al., 2013b) and salt

290   marshes (Hung and Chmura, 2006; Sunderland et al., 2004) in the Bay of Fundy. Over a period

291   of two years (and only one year after the dyke was breached) the concentration of total Hg in the

292   dyke cell was considerably greater (Figure 2). We acknowledge, however, that this dataset has

293   limitations since there were only two replicate cores collected prior to the dyke being breached.

294   Despite this apparent increase, the concentration of Hg in the post-breach sediments had not yet

295   reached that of the salt marsh, which is the target ecosystem. There was a clear decrease in Hg

296   concentration with sediment depth in both the mudflat and the post-breach sediments but not in

297   the salt marsh sediments which is a further indication that the sediment characteristics more

298   closely match the mudflat at this stage of restoration.

299

300   While the total Hg concentrations were greater in the dyke cell after inundation, and the MeHg

301   concentrations were greater at the surface of the sediment, MeHg was observed to be lower

302   overall in the post-breach cores (Figure 2). This lower MeHg concentration was reflected by

303   %MeHg in the sediments of the dyke cell decreasing from 6% pre-breach to 2% post-breach

304   when averaged over all the depths. This observation indicates that methylation has not rapidly

305 occurred in the newly deposited Hg(II) species in the sediment. If the lower MeHg in the post-

306 breach sediments was due to greater export of MeHg from the sediments by tidal flushing then

307 we would have expected to see MeHg depleted in the top few cm of sediment. However, MeHg

308 concentrations were greatest in the top few cm (Figure 2). Therefore, tidal flushing is probably

309 not the reason for the lower MeHg in the post-breach sediments.

310

311 Because total Hg concentrations are greater post-breach and MeHg concentrations are lower, Hg

312 methylation cannot be limited by the supply of total Hg. Hg methylation is rather limited by the

313 bioavailability of Hg to Hg methylating bacteria or the activity of these bacteria (Sunderland et

314 al., 2006). Canário et al. (2007) showed that %MeHg in unvegetated coastal wetland sediments

315 were only 0.6%, while vegetated sediments had up to 18% MeHg. The authors explained that

316 this discrepancy is likely to occur because the presence of vegetation increases microbial activity

317 and favours Hg methylation. Colonisation of the dyke cell by benthic invertebrates (e.g.

318 polychaete worms) may also increase the sediment-water interface and the concentration of

319 MeHg in their burrows (Sizmur et al., 2013a). Therefore, the MeHg concentrations in the dyke

320 cell may increase as the restoration progresses and the dyke cell becomes colonised by

321 vegetation and fauna. This prediction must be contrasted with the observation by Morris et al.

322 (2014) that restored salt marshes have lower MeHg concentrations several decades after

323 inundation when compared to adjacent natural salt marshes. It is therefore unclear whether the

324 MeHg concentration in the dyke cell sediments will increase beyond the concentrations in the

325 adjacent natural salt marsh in the long term.

326

327 *THg concentrations are influenced by soluble carbon, particle size, pH, and salinity but MeHg*

328 *concentrations are poorly predicted*

329 Water-extractable organic carbon, pH, EC, and clay content of sediments all contributed to the

330 multiple linear regression models that explained 52.4% of the variability associated with the

331 concentration of THg, but only 24% of the variability associated with MeHg concentrations in

332 the sediments (Table 2 and Figure 4). Clay content was positively correlated with THg sediment

333 concentration. A reduction in sediment particle size (here observed by an increase in clay

334 content) increases the surface-area-to-volume ratio of particulates in a system. The high surface

335 area and cation exchange capacity of clays results in the adsorption of Hg to fine particles

336 (Bengtsson and Picado, 2008). Suspension of fine sediments in the tidal water increases the

337 likelihood of sediments to scavenge Hg from the water column by settling and retaining Hg in

338 the accumulating sediment (Covelli et al., 2009; Hung and Chmura, 2006; Sunderland et al.,

339 2006). Sediments comprised of fine particles also increase the proportion of particle-bound Hg

340 (Bengtsson and Picado, 2008) and may thus reduce the bioavailability of Hg to methylating

341 bacteria.

342

343 Dissolved organic matter (DOM) is a major binding phase for Hg in aquatic environments

344 (Haitzer et al., 2002; Haverstock et al., 2012; Le Faucheur et al., 2014; O'Driscoll and Evans,

345 2000; Ravichandran, 2004). Here we use WEOC as a proxy for DOM in the sediments following

346 Sizmur et al (2013b). Although we found a positive correlation between THg and both %OM and

347 WEOC, the WEOC explains the THg concentration in the sediments better (Table 2). This

348 observation indicates that the changes in Hg in the sediments are due to a greater fraction that is

349 bound to soluble carbon complexes. The concentration of WEOC in the post-breach sediments

350   (Figure 3) was higher than the mudflat and (unlike the salt marsh) was not associated with

351   vegetation growing in situ. It is therefore likely that the cause of higher concentrations of WEOC

352   (and THg) in the post-breach sediments, compared to the mudflat, is the decaying mat of

353   terrestrial vegetation underneath the freshly deposited sediment. Hg complexation with DOM

354   reduces the bioavailability of Hg to methylating bacteria because the complexes are generally too

355   large to penetrate their biological membranes (Le Faucheur et al., 2014; Ravichandran, 2004).

356   However, soluble organic matter also provides an energy source for methylating bacteria and

357   may increase their activity resulting in greater methylation rates (Ullrich et al., 2001). Further

358   increases in DOM (and microbial activity) are likely to occur as the dyke cell becomes vegetated

359   (Canário et al., 2007) which may increase methylation rates in the future. The deposition of

360   plankton is likely to increase the %MeHg in the fresh sediment as they contain approximately

361   6% to 15% MeHg in the Northwest Atlantic Ocean (Hammerschmidt et al., 2013).

362

363   The solubility and speciation of Hg and the binding of dissolved Hg species to DOM or sediment

364   particles is pH dependent (Gabriel and Williamson, 2004). At low pH, H^+ competes with Hg for

365   binding sites on DOM or the surface of sediment particles, which releases Hg into solution but

366   they also both compete for uptake by negatively charged bacterial cells. In this study pH

367   correlated positively with Hg but negatively with MeHg. This contrast indicates that the greater

368   pH of the mudflat, salt marsh, and post-breach sediments, compared to pre-breach sediments

369   (Figure 3) resulted in greater Hg retention (Hung and Chmura, 2006) but may have reduced Hg

370   bioavailability to methylating bacteria (Barkay et al., 1997; Gilmour and Henry, 1991; Le

371   Faucheur et al., 2014).

372

373   The increase in EC that resulted from the inundation of the dyke cell with sea water (Figure 1c)

374   is due to the high salinity of the seawater (Mouneimne and Price, 2007). The high salinity of the

375   sediment deposited after the dyke cell was inundated with seawater created an environment with

376   a higher ionic strength. As ionic strength increases, the concentration of Hg desorbed into

377   solution decreases (Duarte et al., 1991) resulting in greater Hg retention in sediments and a

378   decrease in the bioavailability of Hg to methylating bacteria (Barkay et al., 1997). Seawater

379   contains high concentrations of chloride ions which can form strong ($\log_{10} K_1^\circ = 7.31$)

380   complexes with mercury species (Powell et al., 2005). The greater the concentration of chloride,

381   the more negatively charged mercuric chloride ions ($HgCl_3^-$ and $HgCl_4^{2-}$) will be present in

382   solution and these negative ions also have a lower bioavailability (Barkay et al., 1997) to

383   methylating bacteria with negatively charged cell walls. Therefore, the increase in ionic strength

384   and formation of trivalent or tetravalent mercuric chloride species in the high EC sediments of

385   the post-breach sediments may have reduced their bioavailability to mercury methylating

386   bacteria. These Hg-chloride complexes may also be less susceptible to photoreduction and loss to

387   the atmosphere (Qureshi et al., 2009).

388

389   In summary, the chemical changes that occur in the sediment after inundation may have

390   impacted on the bioavailability of Hg to methylating bacteria. The decrease in particle size

391   distribution and subsequent increase in sediment surface area may have increased sorption of Hg

392   out of the water column but lowered its bioavailability. Higher organic matter levels may provide

393   a food source for methylating bacteria and increase their activity. Greater soluble organic carbon

394   may mobilise Hg from the surface of sediments but also complex it in a form that is unavailable

395   to methylating bacteria. An increase in sediment pH increases the concentration that can be

396 adsorbed from the solution phase and reduces the bioavailability. Finally, the higher ionic

397 strength leads to a greater proportion of inorganic complexes and a lower bioavailability of Hg.

398 This final conclusion assumes that the uptake of Hg by methylating bacteria occurs by passive

399 diffusion of neural or ionic lipophilic Hg species but there is now a considerable body of

400 evidence to suggest that uptake may occur by facilitated diffusion or active transportation by

401 protein pumps (Hsu-Kim et al., 2013).

402

403 *Conclusions and Implications for Coastal Managed Retreat*

404 Despite a doubling of Hg concentration within the dyke cell after the dyke was breached, Hg

405 concentrations are still below the Canadian Sediment Quality Guidelines (CCME, 2002). The

406 reason for the Hg increase in this study was the fresh deposition of sediments with a smaller

407 particle size distribution that are able to scavenge and retain Hg due to their higher surface area,

408 negative charge, and higher pH. This site can therefore be considered a net sink for mercury

409 during the first year after the dyke was breached. The more sediment that is deposited, the larger

410 the sink will become. In contrast to considerable increases in mercury methylation observed

411 during freshwater wetland creation (Kelly et al., 1997; Sinclair et al., 2012), we observed a 27%

412 decrease in MeHg concentrations in the dyke cell after the dyke was breached. This decrease

413 may have been due to greater Hg retention and lower Hg bioavailability to methylating bacteria

414 but ultimately cannot be fully explained with the available data and is limited by the low number

415 of replicate cores collected. Further work will be required to explain the precise mechanisms for

416 this decrease.

417

418   Our data provides no evidence for a flush of Hg methylation during the first year of managed

419   retreat. As the restoration progresses and vegetation colonises, the soluble carbon concentration

420   and microbial activity may increase and the rate of Hg methylation may also increase. However,

421   contradictory data from other studies indicate that it is unclear whether MeHg will be elevated

422   beyond the concentration found in natural wetlands (Canário et al., 2007; Kelly et al., 1997;

423   Morris et al., 2014; Sinclair et al., 2012). We conclude that coastal flooding of sediments subject

424   to diffuse Hg contamination during managed retreat of coastal flood defences does not pose a

425   significant risk of increasing Hg methylation or bioavailability during the first year.

426

431

432   **References**

433   Barkay, T., Gillman, M., Turner, R.R., 1997. Effects of dissolved organic carbon and salinity on

434   bioavailability of mercury. Applied and environmental microbiology 63, 4267-4271.

435   Bengtsson, G., Picado, F., 2008. Mercury sorption to sediments: Dependence on grain size,

436   dissolved organic carbon, and suspended bacteria. Chemosphere 73, 526-531.

437   Byers, S.C., Mills, E.L., Stewart, P.L., 1978. A comparison of methods of determining organic

438   carbon in marine sediments, with suggestions for a standard method. Hydrobiologia 58, 43-47.

439   Canário, J., Caetano, M., Vale, C., Cesário, R., 2007. Evidence for elevated production of

440   methylmercury in salt marshes. Environmental science & technology 41, 7376-7382.

441   CCME, 2002. Canadian Sediment Quality Guidelines for the Protection of Aquatic Life.

442   Compeau, G., Bartha, R., 1985. Sulfate-reducing bacteria: principal methylators of mercury in

443   anoxic estuarine sediment. Applied and environmental microbiology 50, 498-502.

444   Covelli, S., Acquavita, A., Piani, R., Predonzani, S., De Vittor, C., 2009. Recent contamination

445   of mercury in an estuarine environment (Marano lagoon, Northern Adriatic, Italy). Estuarine,

446   Coastal and Shelf Science 82, 273-284.

447   Crowell, N., Webster, T., O'Driscoll, N.J., 2011. GIS modelling of intertidal wetland exposure

448   characteristics. Journal of Coastal Research 27, 44-51.

449   Desplanque, C., Mossman, D.J., 2004. Tides and their seminal impact on the geology,

450   geography, history, and socio-economics of the Bay of Fundy, eastern Canada. Atlantic Geology

451   40.

452   Duarte, A., Pereira, M., Oliveira, J., Hall, A., 1991. Mercury desorption from contaminated

453   sediments. Water Air & Soil Pollution 56, 77-82.

454   Emmerson, R., Birkett, J., Scrimshaw, M., Lester, J., 2000. Solid phase partitioning of metals in

455   managed retreat soils: field changes over the first year of tidal inundation. Science of the Total

456   Environment 254, 75-92.

457   Evers, D.C., Han, Y.-J., Driscoll, C.T., Kamman, N.C., Goodale, M.W., Lambert, K.F., Holsen,

458   T.M., Chen, C.Y., Clair, T.A., Butler, T., 2007. Biological mercury hotspots in the northeastern

459   United States and southeastern Canada. Bioscience 57, 29-43.

460   Gabriel, M.C., Williamson, D.G., 2004. Principal biogeochemical factors affecting the speciation

461   and transport of mercury through the terrestrial environment. Environmental geochemistry and

462   health 26, 421-434.

463   Gilmour, C.C., Henry, E.A., 1991. Mercury methylation in aquatic systems affected by acid

464   deposition. Environmental Pollution 71, 131-169.

465 Gordon Jr, D.C., Baretta, J.W., 1982. A preliminary comparison of two turbid coastal

466 ecosystems: The Dollard (Netherlands-FRG) and the Cumberland Basin (Canada).

467 Hydrobiological Bulletin 16, 255-267.

468 Guédron, S., Huguet, L., Vignati, D., Liu, B., Gimbert, F., Ferrari, B., Zonta, R., Dominik, J.,

469 2012. Tidal cycling of mercury and methylmercury between sediments and water column in the

470 Venice Lagoon (Italy). Marine Chemistry 130, 1-11.

471 Haitzer, M., Aiken, G.R., Ryan, J.N., 2002. Binding of mercury (II) to dissolved organic matter:

472 the role of the mercury-to-DOM concentration ratio. Environmental science & technology 36,

473 3564-3570.

474 Hammerschmidt, C.R., Finiguerra, M.B., Weller, R.L., Fitzgerald, W.F., 2013. Methylmercury

475 accumulation in plankton on the continental margin of the northwest atlantic ocean.

476 Environmental science & technology 47, 3671-3677.

477 Haverstock, S., Sizmur, T., Murimboh, J., O'Driscoll, N.J., 2012. Modeling the photo-oxidation

478 of dissolved organic matter by ultraviolet radiation in freshwater lakes: Implications for mercury

479 bioavailability. Chemosphere 88, 1220-1226.

480 Heim, W.A., Coale, K.H., Stephenson, M., Choe, K.-Y., Gill, G.A., Foe, C., 2007. Spatial and

481 habitat-based variations in total and methyl mercury concentrations in surficial sediments in the

482 San Francisco Bay-Delta. Environmental science & technology 41, 3501-3507.

483 Hsu-Kim, H., Kucharzyk, K.H., Zhang, T., Deshusses, M.A., 2013. Mechanisms Regulating

484 Mercury Bioavailability for Methylating Microorganisms in the Aquatic Environment: A Critical

485 Review. Environmental science & technology 47, 2441-2456.

486 Hung, G.A., Chmura, G.L., 2006. Mercury accumulation in surface sediments of salt marshes of

487 the Bay of Fundy. Environmental Pollution 142, 418-431.

488 Kelly, C., Rudd, J., Bodaly, R., Roulet, N., St. Louis, V., Heyes, A., Moore, T., Schiff, S.,

489 Aravena, R., Scott, K., 1997. Increases in fluxes of greenhouse gases and methyl mercury

490 following flooding of an experimental reservoir. Environmental science & technology 31, 1334-

491 1344.

492 Lavoie, R.A., Hebert, C.E., Rail, J.-F., Braune, B.M., Yumvihoze, E., Hill, L.G., Lean, D.R.,

493 2010. Trophic structure and mercury distribution in a Gulf of St. Lawrence (Canada) food web

494 using stable isotope analysis. Science of the Total Environment 408, 5529-5539.

495 Le Faucheur, S., Campbell, P.G.C., Fortin, C., Slaveykova, V.I., 2014. Interactions between

496 mercury and phytoplankton: Speciation, bioavailability, and internal handling. Environmental

497 Toxicology and Chemistry 33, 1211-1224.

498 Miller, W., Miller, D., 1987. A micro-pipette method for soil mechanical analysis.

499 Communications in Soil Science & Plant Analysis 18, 1-15.

500 Morris, M.A., Spencer, K.L., Belyea, L.R., Branfireun, B.A., 2014. Temporal and spatial

501 distributions of sediment mercury in restored coastal saltmarshes. Marine Chemistry 167, 150-

502 159.

503 Mouneimne, S.M., Price, J.S., 2007. Seawater contamination of a harvested bog: hydrological

504 aspects. Wetlands 27, 355-365.

505 O'Driscoll, N.J., Evans, R.D., 2000. Analysis of methyl mercury binding to freshwater humic

506 and fulvic acids by gel permeation chromatography/hydride generation ICP-MS. Environmental

507 science & technology 34, 4039-4043.

508 O'Driscoll, N.J., Canário, J., Crowell, N., Webster, T., 2011. Mercury speciation and distribution

509 in coastal wetlands and tidal mudflats: relationships with sulphur speciation and organic carbon.

510 Water, Air, & Soil Pollution 220, 313-326.

511 Ollerhead, J., Spicer, C., Bams, R., 2011. Monitoring a salt marsh restoration at Fort Beausejour,

512 Aulac, NB - Final Report, Ducks Unlimited Canada.

513 Portnoy, J., Giblin, A., 1997. Effects of historic tidal restrictions on salt marsh sediment

514 chemistry. Biogeochemistry 36, 275-303.

515 Powell, K.J., Brown, P.L., Byrne, R.H., Gajda, T., Hefter, G., Sjöberg, S., Wanner, H., 2005.

516 Chemical speciation of environmentally significant heavy metals with inorganic ligands. Part 1:

517 The Hg^{2+}–Cl^-, OH^-, CO_3^{2-}, SO_4^{2-}, and PO_4^{3-} aqueous systems (IUPAC Technical Report).

518 Pure and applied chemistry 77, 739-800.

519   Qureshi, A., O'Driscoll, N.J., MacLeod, M., Neuhold, Y.-M., Hungerbühler, K., 2009.

520   Photoreactions of mercury in surface ocean water: gross reaction kinetics and possible pathways.

521   Environmental science & technology 44, 644-649.

522   Rasmussen, R.S., Nettleton, J., Morrissey, M.T., 2005. A review of mercury in seafood: Special

523   focus on tuna. Journal of Aquatic Food Product Technology 14, 71-100.

524   Ravichandran, M., 2004. Interactions between mercury and dissolved organic matter—a review.

525   Chemosphere 55, 319-331.

526   Sinclair, K.A., Xie, Q., Mitchell, C.P., 2012. Methylmercury in water, sediment, and

527   invertebrates in created wetlands of Rouge Park, Toronto, Canada. Environmental Pollution 171,

528   207-215.

529   Singh, K., Walters, B.B., Ollerhead, J., 2007. Climate change, sea-level rise and the case for salt

530   marsh restoration in the Bay of Fundy, Canada. Environments: a journal of interdisciplinary

531   studies 35.

532   Sizmur, T., Canário, J., Edmonds, S., Godfrey, A., O'Driscoll, N.J., 2013a. The polychaete worm

533   Nereis diversicolor increases mercury lability and methylation in intertidal mudflats.

534   Environmental Toxicology and Chemistry 32, 1888-1895.

535   Sizmur, T., Canário, J., Gerwing, T.G., Mallory, M.L., O'Driscoll, N.J., 2013b. Mercury and

536   methylmercury bioaccumulation by polychaete worms is governed by both feeding ecology and

537   mercury bioavailability in coastal mudflats. Environmental Pollution 176, 18-25.

538   Sizmur, T., Palumbo-Roe, B., Hodson, M.E., 2011. Impact of earthworms on trace element

539   solubility in contaminated mine soils amended with green waste compost. Environmental

540   Pollution 159, 1852-1860.

541   Sunderland, E.M., Amirbahman, A., Burgess, N.M., Dalziel, J., Harding, G., Jones, S.H., Kamai,

542   E., Karagas, M.R., Shi, X., Chen, C.Y., 2012. Mercury sources and fate in the Gulf of Maine.

543   Environmental research 119, 27-41.

544   Sunderland, E.M., Gobas, F.A., Branfireun, B.A., Heyes, A., 2006. Environmental controls on

545   the speciation and distribution of mercury in coastal sediments. Marine Chemistry 102, 111-123.

546   Sunderland, E.M., Gobas, F.A., Heyes, A., Branfireun, B.A., Bayer, A.K., Cranston, R.E.,

547   Parsons, M.B., 2004. Speciation and bioavailability of mercury in well-mixed estuarine

548   sediments. Marine Chemistry 90, 91-105.

549   U.S.EPA, 1998. Method 7473: Mercury in solids and solutions by thermal decomposition,

550   amalgamation and atomic spectrophotometry, U.S. Environmental Protection Agency,

551   Washington, DC.

552   Ullrich, S.M., Tanton, T.W., Abdrashitova, S.A., 2001. Mercury in the aquatic environment: a

553   review of factors affecting methylation. Critical Reviews in Environmental Science and

554   Technology 31, 241-293.

555   Williams, P.B., Orr, M.K., 2002. Physical evolution of restored breached levee salt marshes in

556   the San Francisco Bay estuary. Restoration Ecology 10, 527-542.

557   Wynn, G., 1979. Late eighteenth-century agriculture on the Bay of Fundy marshlands.

558   Acadiensis, 80-89.

559

560